

ORIGINAL INVESTIGATIONS

Markers of Myocardial Damage Predict Mortality in Patients With Aortic Stenosis



Soongu Kwak, MD,^a Russell J. Everett, MD, PhD,^b Thomas A. Treibel, MD, PhD,^c Seokhun Yang, MD,^a Doyeon Hwang, MD,^a Taehoon Ko, PhD,^d Michelle C. Williams, MD, PhD,^b Rong Bing, MD,^b Trisha Singh, BM,^b Shruti Joshi, MBBS,^b Heesun Lee, MD,^a Whal Lee, MD, PhD,^e Yong-Jin Kim, MD, PhD,^a Calvin W.L. Chin, MD, PhD,^f Miho Fukui, MD, PhD,^g Tarique Al Musa, MD,^h Marzia Rigolli, MD,ⁱ Anvesha Singh, MBCB,^j Lionel Tastet, MSc,^k Laura E. Dobson, MD,^h Stephanie Wiesemann, MD,^l Vanessa M. Ferreira, MD, DPHL,ⁱ Gabriella Captur, MD, PhD,^m Sahmin Lee, MD, PhD,ⁿ Jeanette Schulz-Menger, MD,^l Erik B. Schelbert, MD,^o Marie-Annick Clavel, DVM, PhD,^k Sung-Ji Park, MD, PhD,^p Tobias Rheude, MD,^q Martin Hadamitzky, MD,^r Bernhard L. Gerber, MD, PhD,^s David E. Newby, MD, PhD,^b Saul G. Myerson, MD,ⁱ Phillippe Pibarot, DVM, PhD,^k João L. Cavalcante, MD,^o Gerry P. McCann, MBCB,^j John P. Greenwood, MD, PhD,^h James C. Moon, MD,^c Marc R. Dweck, MD, PhD,^{b,*} Seung-Pyo Lee, MD, PhD^{a,t,*}

ABSTRACT

BACKGROUND Cardiovascular magnetic resonance (CMR) is increasingly used for risk stratification in aortic stenosis (AS). However, the relative prognostic power of CMR markers and their respective thresholds remains undefined.

OBJECTIVES Using machine learning, the study aimed to identify prognostically important CMR markers in AS and their thresholds of mortality.

METHODS Patients with severe AS undergoing AVR ($n = 440$, derivation; $n = 359$, validation cohort) were prospectively enrolled across 13 international sites (median 3.8 years' follow-up). CMR was performed shortly before surgical or transcatheter AVR. A random survival forest model was built using 29 variables (13 CMR) with post-AVR death as the outcome.

RESULTS There were 52 deaths in the derivation cohort and 51 deaths in the validation cohort. The 4 most predictive CMR markers were extracellular volume fraction, late gadolinium enhancement, indexed left ventricular end-diastolic volume (LVEDVi), and right ventricular ejection fraction. Across the whole cohort and in asymptomatic patients, risk-adjusted predicted mortality increased strongly once extracellular volume fraction exceeded 27%, while late gadolinium enhancement $>2\%$ showed persistent high risk. Increased mortality was also observed with both large ($LVEDVi > 80 \text{ mL/m}^2$) and small ($LVEDVi \leq 55 \text{ mL/m}^2$) ventricles, and with high ($>80\%$) and low ($\leq 50\%$) right ventricular ejection fraction. The predictability was improved when these 4 markers were added to clinical factors (3-year C-index: 0.778 vs 0.739). The prognostic thresholds and risk stratification by CMR variables were reproduced in the validation cohort.

CONCLUSIONS Machine learning identified myocardial fibrosis and biventricular remodeling markers as the top predictors of survival in AS and highlighted their nonlinear association with mortality. These markers may have potential in optimizing the decision of AVR. (J Am Coll Cardiol 2021;78:545-558) Crown Copyright © 2021 Published by Elsevier on behalf of the American College of Cardiology Foundation. All rights reserved.



Listen to this manuscript's audio summary by
Editor-in-Chief
Dr. Valentin Fuster on
JACC.org.

From the ^aDepartment of Internal Medicine, Seoul National University Hospital, Seoul, South Korea; ^bBritish Heart Foundation Centre for Cardiovascular Science, University of Edinburgh, Edinburgh, United Kingdom; ^cBarts Health NHS Trust and University College London, London, United Kingdom; ^dOffice of Hospital Information, Seoul National University Hospital, Seoul, Korea; ^eDepartment of Radiology, Seoul National University Hospital, Seoul, Korea; ^fNational Heart Center Singapore, Singapore; ^gCardiovascular Imaging Research Center and Core Lab, Minneapolis Heart Institute Foundation, Minneapolis, Minnesota, USA; ^hMultidisciplinary Cardiovascular Research Centre & The Division of Biomedical Imaging, Leeds Institute for Cardiovascular and

ABBREVIATIONS AND ACRONYMS

AS	= aortic stenosis
AVR	= aortic valve replacement
CI	= confidence interval
CMR	= cardiovascular magnetic resonance
ECV%	= extracellular volume fraction
HR	= hazard ratio
IQR	= interquartile range
LGE	= late gadolinium enhancement
LV	= left ventricular
LVEDVi	= indexed left ventricular end-diastolic volume
LVEF	= left ventricular ejection fraction
NYHA	= New York Heart Association
RSF	= random survival forest
RV	= right ventricular
RVEF	= right ventricular ejection fraction
SAVR	= surgical aortic valve replacement
TAVR	= transcatheter aortic valve replacement

Aortic stenosis (AS) is a major health burden in aging societies. Although aortic valve replacement (AVR) provides definite treatment for the valve, prognosis remains poor once irreversible myocardial damage develops (1). Therefore, early detection of ventricular decompensation in AS is important, with efforts to find novel imaging biomarkers ongoing.

There is a growing interest in cardiovascular magnetic resonance (CMR) as a complementary prognostic tool. CMR provides detailed information on biventricular structure, function, and myocardial fibrosis; both diffuse fibrosis using T1-mapping (eg, extracellular volume fraction [ECV%]) and replacement fibrosis using late gadolinium enhancement (LGE) demonstrate important prognostic information (2-9). However, these myocardial fibrosis assessments are collinear and associated with other imaging and clinical factors already used for prognostication (2-9). It remains unclear how powerful these CMR markers of myocardial damage are in comparison with standard clinical and echocardiographic parameters, nor what thresholds best predict prognosis and might be used to help optimize the timing of AVR. Such analysis is challenging using traditional regression analyses, which are limited by multicollinearity (10). In contrast, machine learning can assess the predictive hierarchy of variables and provide powerful feature extraction techniques (10-14), with random survival forest (RSF) particularly useful for delineating nonlinear associations (10-13).

We hypothesized that RSF machine learning would provide novel insights into the predictors of death in patients with severe AS undergoing AVR, and that this data-driven approach would stratify the relative importance of myocardial damage markers and identify clinically relevant nonlinear threshold effects.

SEE PAGE 559

METHODS

The analysis pipeline (data-driven feature discovery) is depicted in the [Central Illustration](#). Briefly, we first identified important CMR predictors for post-AVR mortality in the RSF model. Next, the nonlinear association of these CMR markers with mortality and their thresholds were examined using the partial dependency plot. Finally, using the thresholds from the partial plots, the clinical implication and utility of these CMR markers were sought. More detail of the Methods is available in the [Supplemental Methods](#).

STUDY DESIGN. Two separate datasets were gathered, a derivation cohort for the development of a machine learning prediction model ($n = 440$) and a validation cohort for external validation ($n = 359$) ([Supplemental Methods](#), [Supplemental Table 1](#)). Both datasets included patients with severe AS awaiting AVR, with CMR performed shortly before AVR. The derivation cohort was recruited from 10 international sites (6) and the validation cohort from 5 international sites. Patients were recruited regardless of aortic valve morphology (bicuspid or tricuspid) or the type of intervention received (surgical aortic valve replacement [SAVR] with or without coronary artery bypass grafting or transcatheter aortic valve replacement [TAVR]).

Metabolic Medicine, University of Leeds, Leeds, United Kingdom; ¹University of Oxford Centre for Clinical Magnetic Resonance Research, BHF Centre of Research Excellence (Oxford), NIHR Biomedical Research Centre (Oxford), Oxford, United Kingdom; ²Department of Cardiovascular Sciences, Glenfield Hospital, University of Leicester and NIHR Leicester Biomedical Research Centre, Leicester, United Kingdom; ³Institut Universitaire de Cardiologie et de Pneumologie de Québec/Québec Heart and Lung Institute, Université Laval, Québec City, Québec, Canada; ⁴Charité Campus Buch ECRC and Helios Clinics Cardiology Germany, DZHK partner site, Berlin, Germany; ⁵Inherited Heart Muscle Disease Clinic, Department of Cardiology, Royal Free Hospital, NHS Foundation Trust, London, United Kingdom; ⁶Division of Cardiology, Asan Medical Center Heart Institute, University of Ulsan College of Medicine, Seoul, South Korea; ⁷UPMC Cardiovascular Magnetic Resonance Center, Heart and Vascular Institute, University of Pittsburgh Medical Center, Pittsburgh, Pennsylvania, USA; ⁸Division of Cardiology, Department of Medicine, Cardiovascular Imaging Center, Heart Vascular Stroke Institute, Samsung Medical Center, Sungkyunkwan University School of Medicine, Seoul, South Korea; ⁹Department of Cardiology, German Heart Center Munich, Munich, Germany; ¹⁰Department of Radiology and Nuclear Medicine, German Heart Center Munich, Munich, Germany; ¹¹Division of Cardiology, Department of Cardiovascular Diseases, Cliniques Universitaires St. Luc and Institut de Recherche Cardiovasculaire, Université Catholique de Louvain, Brussels, Belgium; and the ¹²Center for Precision Medicine, Seoul National University Hospital, Seoul, South Korea. *Drs Dweck and Lee contributed equally to this work.

The authors attest they are in compliance with human studies committees and animal welfare regulations of the authors' institutions and Food and Drug Administration guidelines, including patient consent where appropriate. For more information, visit the [Author Center](#).

Manuscript received April 15, 2021; revised manuscript received May 7, 2021, accepted May 10, 2021.

Severe AS was ascertained by echocardiography at each center. CMR assessments of biventricular volume, function, left atrial size, and left ventricular (LV) mass index were used, given its greater accuracy. The study complied with the Declaration of Helsinki, and local Institutional Review Boards approved the study protocol. All participants provided written informed consent.

CARDIOVASCULAR MAGNETIC RESONANCE. All participants underwent CMR shortly before AVR (6). T1-mapping was performed according to a standardized prespecified protocol in the mid inferoseptum (6). Infarct-related LGE was excluded from T1-mapping regions of interest, whereas noninfarct LGE was included (15). ECV% was calculated conventionally using hematocrit and pre- and post-gadolinium blood and myocardial T1 values (16). The details of scanners, T1-mapping sequences, and field strengths by each center are summarized ([Supplemental Methods](#), [Supplemental Table 2](#), [Supplemental Figure 1](#)). Briefly, native T1 values varied substantially across the centers, mainly owing to the difference in the magnetic field strength. In contrast, ECV% values were similar across the study centers regardless of the field strength, supporting its generalizability.

OUTCOME ASSESSMENT. The primary endpoint was all-cause mortality. Mortality was ascertained by national or medical death records, or reports from family members. Patients were followed from the date of AVR to the last clinical follow-up or death.

VARIABLES USED FOR THE ANALYSIS. We included 29 variables (12 demographic or clinical, 4 echocardiographic, and 13 CMR) ([Supplemental Table 3](#)) for the RSF analysis. As the main objective was to investigate the prognostic hierarchy of myocardial damage markers assessed by CMR, we included biventricular structural and functional parameters of CMR and 2 myocardial fibrosis markers (ECV% and percentage of LGE [LGE%]) (2–9). Additionally, we included clinical and echocardiographic parameters used in routine practice and known to be associated with adverse outcomes in severe AS, including baseline characteristics (eg, age, sex, systolic or diastolic blood pressure), comorbidities (eg, atrial fibrillation, myocardial infarction), surgical factors (eg, intervention type), and echocardiographic indices of AS severity (peak aortic valve velocity, mean pressure gradient, aortic valve area index, and valvuloarterial impedance) (17,18).

The proportion of missing values was minimal ([Supplemental Figure 2](#)), and these were imputed using the *missForest* algorithm before the analysis.

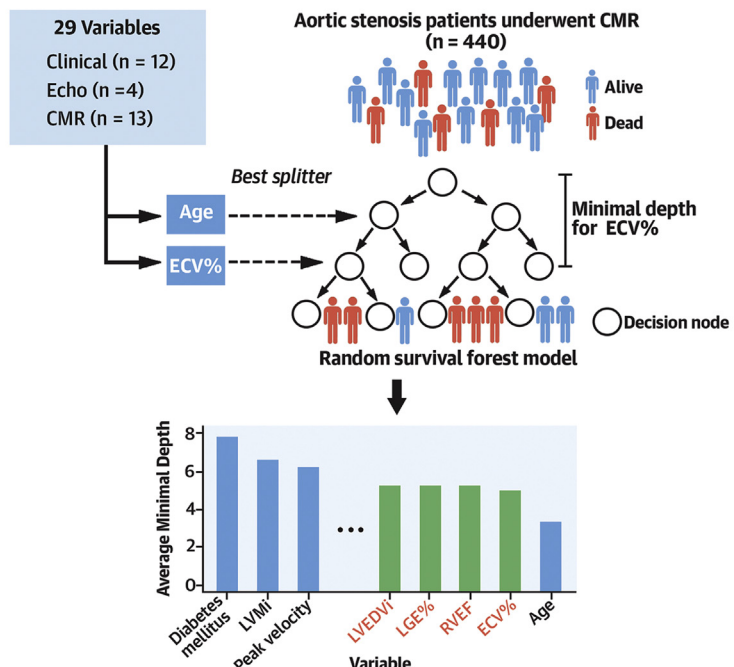
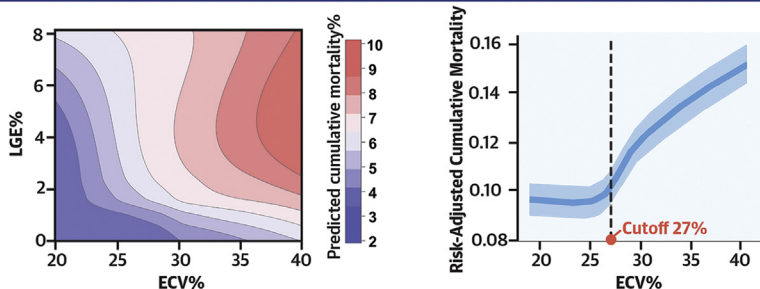
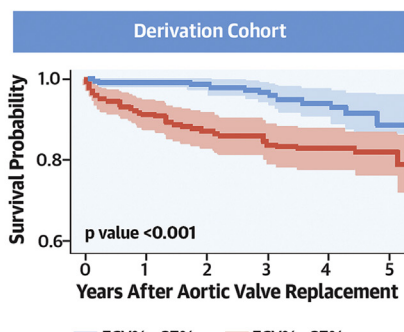
RSF ANALYSIS. The RSF model for all-cause mortality was built with 29 variables using the derivation cohort. In RSF analyses, each decision tree is trained with a bootstrapping sample from the entire cohort (19). The tree is started from the trunk, and a random set of variables is selected to split it into 2 branches, maximizing the log-rank statistics (19). In this study, 5 random variables were considered at each split. The ensemble of 2,000 decision trees generated the final RSF model.

After developing the RSF model, we ranked the 29 variables by their prognostic capability using minimal depth (11–13,20). Minimal depth is defined as the shortest distance from the tree trunk to the node of a specific variable, with smaller minimal depths indicating greater significance (20). Thus, we focused on the CMR variables that presented the smallest minimal depths.

PREDICTIVE BEHAVIOR AND RELATIONSHIP OF THE MYOCARDIAL CMR VARIABLES. Next, we examined the predictive behaviors or associations of the most predictive CMR variables on outcome. To delineate nonlinear effects, we took advantage of partial dependency plots derived from the RSF model (10–12). While dependency plots show the unadjusted overall trend of the predicted mortality in relation to a variable (eg, ECV%) (13), partial dependency plots show the association adjusted for all other variables included in the respective RSF model, thus displaying the nonlinear effect of the variable on the outcome (10–12). Partial dependency plots were drawn with each observation as a point, traced by LOESS curves.

VALIDATION OF THE NONLINEAR ASSOCIATIONS AND THRESHOLDS FROM THE RSF ANALYSIS. We conducted the following analyses to validate the nonlinear associations and thresholds observed on the partial plots, using both derivation and validation cohorts ([Supplemental Methods](#)): 1) Kaplan-Meier survival analysis using the thresholds identified on the partial plots (derivation and validation cohorts); 2) verifying the incremental predictive information provided by the CMR variables when added to risk prediction models based on clinical risk factors (model development in the derivation cohort, tested in the validation cohort); and 3) analysis of whether combining the CMR predictors into an AS-CMR risk score, defined as the total number of abnormal CMR features, provides effective risk stratification (derivation and validation cohorts).

STATISTICAL ANALYSIS. Continuous variables are presented as median (interquartile range [IQR]) and categorical variables as frequency and percentage.

CENTRAL ILLUSTRATION Unbiased Feature Discovery Using RSF
A. Discovery and Ranking of Prognostically Important CMR Markers

B. Non-Linear Associations of CMR Markers with All-Cause Death

C. Validation of Thresholds for Each CMR Marker


- Derivation cohort (n = 440)
Adjusted hazard ratio (95% CI): 2.29 (1.20-4.37), p = 0.012

- Findings confirmed in the validation cohort (n = 359)
Adjusted hazard ratio (95% CI): 2.80 (1.47-5.33), p = 0.002

Differences between groups were compared with Student's *t*-test or Wilcoxon's rank sum test for continuous variables and chi-square test or Fisher exact test for categorical variables. Kaplan-Meier survival analysis was performed with the duration from the AVR to the last follow-up or death and compared with the log-rank test. Multivariable Cox models included the variables that were significant in the univariable Cox analysis and known clinical risk factors: age, sex, atrial fibrillation, and intervention type. These same variables were also considered as important ones by minimal depths in the RSF analysis, except for sex (Figure 1). Cox proportional hazards assumption was tested using global Schoenfeld residuals, and the time-varying effect of a variable on the outcome was analyzed. The predictability of Cox and RSF models was calculated as Harrell's C-index from the validation set.

A 2-sided *P* value <0.05 was considered statistically significant. All analysis was done with R version 3.6.0 (R Foundation for Statistical Computing, Vienna, Austria) (Supplemental Table 4).

RESULTS

STUDY POPULATION. The derivation cohort comprised 440 patients (70 ± 10 years of age, 58.9% male), in whom AVR was performed shortly following CMR (median 15 days [IQR: 4–58 days]). A total of 144 (32.7%) patients had a bicuspid aortic valve, and 29 (6.6%) patients had low-flow, low-gradient AS with either reduced ($n = 20$) or preserved ($n = 9$) ejection fraction. Regarding intervention type, 311 (71%) patients underwent SAVR, 62 (14%) underwent combined SAVR with coronary artery bypass grafting, and 67 (15%) underwent TAVR. Patients undergoing TAVR were older and had higher Society of Thoracic Surgeons scores (Supplemental Table 5).

During a median follow-up of 3.8 years (IQR: 2.9–4.6 years), there were 52 deaths. Patients who died were older, predominantly male, and more symptomatic at the time of AVR (Table 1). Mortality was lower in patients who underwent isolated SAVR

compared with other forms of intervention (Supplemental Figure 3). Regarding CMR parameters, those who died had higher ECV%, more LGE%, larger left atrial volumes, and lower LV ejection fraction (LVEF) and right ventricular ejection fraction (RVEF) than did those who did not (Table 1).

Compared with the derivation cohort, an independent validation cohort ($n = 359$) comprised more elderly patients (mean 73 years of age vs 70 years of age; $P < 0.001$) and had a higher proportion of patients who underwent TAVR (30.6% vs 15.2%; $P < 0.001$). There were 51 deaths in the validation cohort during a median follow-up of 3.3 years (IQR: 1.4–4.9 years), with nonsignificantly lower survival than the derivation cohort ($P = 0.183$) (Supplemental Methods and Supplemental Table 1).

RELATIVE VARIABLE IMPORTANCE IN THE RSF MODEL.

In the RSF model built with all 29 variables using the derivation cohort, the most important factor was age (minimal depth 3.32) (Figure 1). Atrial fibrillation (5.21) emerged as an important clinical risk factor, but other comorbidities such as myocardial infarction (6.92) and diabetes mellitus (7.79) had relatively high minimal depths, as did echocardiographic AS severity indices (peak velocity 6.20, aortic valve area index 6.44), indicating little predictive value.

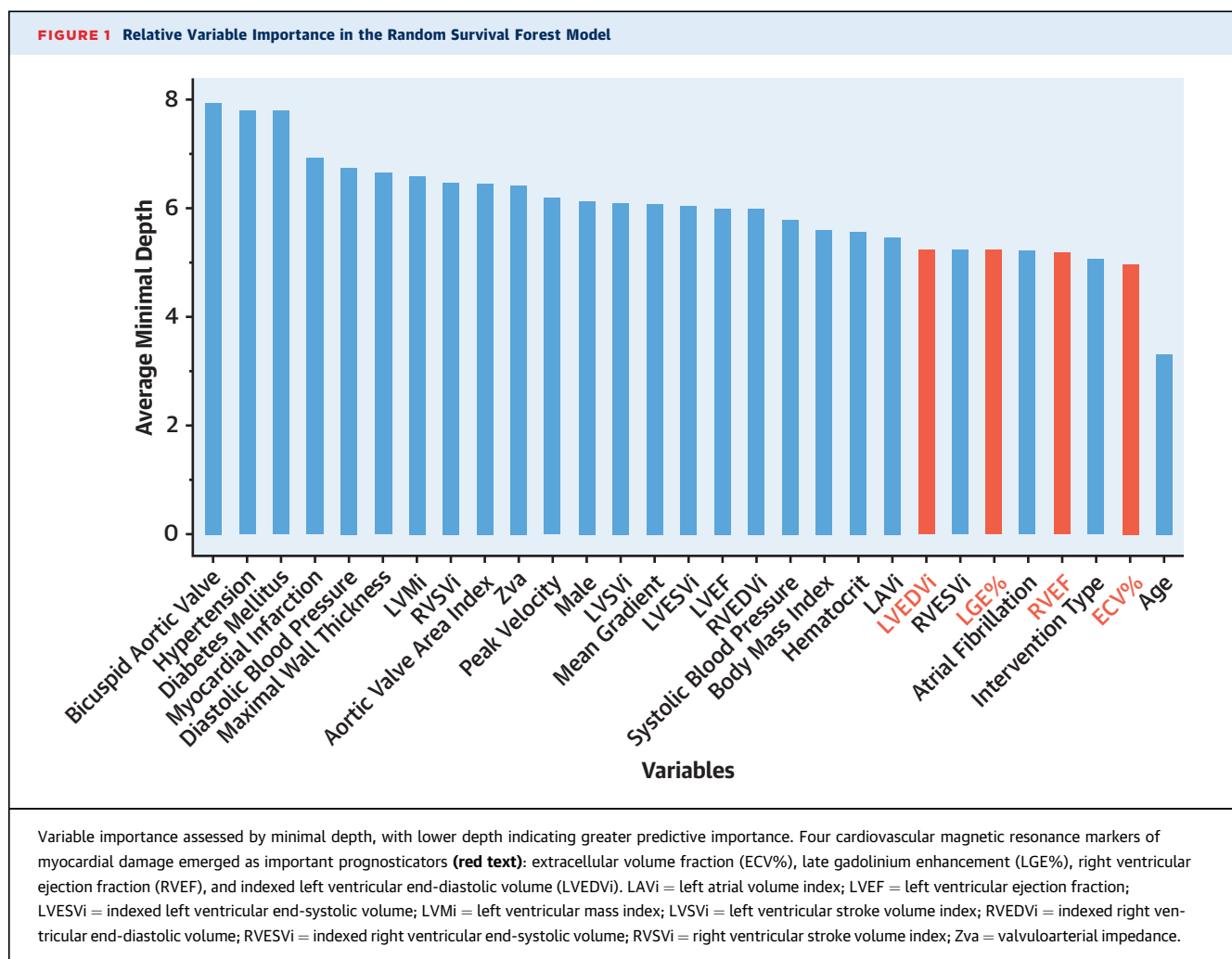
Regarding CMR parameters, ECV% was the second most powerful predictor among all variables (4.96). The RVEF (5.18), LGE% (5.22), indexed LV end-diastolic volume (LVEDVi), and indexed RV end-systolic volume (both 5.23) were also predictors with lower minimal depth (Figure 1). However, more commonly recognized LV remodeling and functional measures in AS, such as LVEF (6.00) and LV mass index (6.58), offered comparatively little predictive information.

VARIABLE DEPENDENCY AND PARTIAL DEPENDENCY IN THE RSF MODEL.

We generated nonadjusted variable dependency plots for the 4 most predictive CMR variables of myocardial health in the RSF model using 3-year mortality risk (Supplemental Figure 4). The

CENTRAL ILLUSTRATION Continued

(A) The random survival forest (RSF) model for post-aortic valve replacement (AVR) death was constructed using 29 variables. Minimal depth was used to rank the variable importance. Four myocardial cardiovascular magnetic resonance (CMR) markers emerged as important markers (extracellular volume fraction [ECV%], late gadolinium enhancement [LGE%], right ventricular ejection fraction [RVEF], indexed left ventricular end-diastolic volume [LVEDVi]). (B) Association between variables and mortality was examined using partial dependency plots, which are generated by averaging out the effects of all other variables. A partial co-plot between ECV% and LGE% is depicted (left). A nonlinear effect of ECV% was identified, with a clear risk threshold (>27%) (right). (C) Threshold verified in Kaplan-Meier curves, confirming the generalizability and potential utility of ECV%.



indexed RV end-systolic volume was omitted because of its high correlation with RVEF (Pearson's $r = -0.82$). In these nonadjusted models, the predicted 3-year survival became lower as ECV% increased, LVEDVi increased, and RVEF decreased. There was a negative correlation between LGE% and survival.

Next, we examined partial dependency plots, which demonstrate the adjusted variable dependencies after integrating out the effects of all other variables (Figure 2). On these plots, each variable demonstrated distinct nonlinear behaviors not previously apparent with the conventional regression analyses. Although ECV% demonstrated a minimal effect on predicted mortality below 27%, mortality increased steeply once ECV% exceeded 27%. Predicted mortality also increased with LGE: rising as LGE% increased up to 2%, with a plateau of elevated risk thereafter. There was a nonlinear relationship between mortality and LVEDVi, with small ($\leq 55 \text{ mL/m}^2$) and large ($> 80 \text{ mL/m}^2$) ventricles both associated with increased

mortality. The RVEF showed a similar pattern, with RVEF $> 80\%$ and $\leq 50\%$ associated with higher mortality. Partial plots of the 4 most predictive clinical factors in the RSF model (age, intervention type, atrial fibrillation, and hematocrit) are shown in Supplemental Figure 5.

In internal validation analyses, the relative variable importance of these 4 CMR variables and their nonlinear associations with mortality (partial plots) were consistent in both the 100 randomly generated replicates and 10-fold cross-validation by participating centers (Supplemental Figures 6 and 7). Sensitivity analysis using the derivation and validation cohort combined as a single training dataset also yielded similar results, supporting the robustness of these findings (Supplemental Figure 8). The shape of the partial plots of the 4 CMR parameters was similar across the intervention type, with consistent nonlinear effects and cutoffs (eg, ECV% $> 27\%$) (Supplemental Figure 9).

TABLE 1 Baseline Characteristics of the Participants in the Derivation Cohort

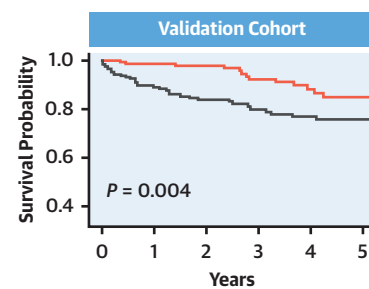
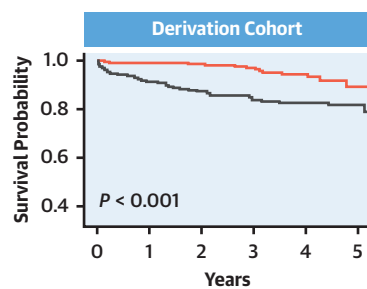
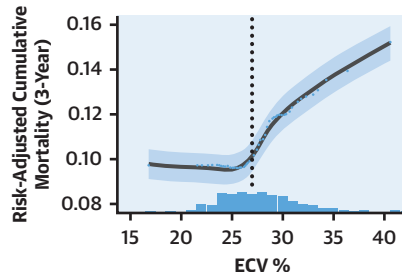
	Alive (n = 388)	Dead (n = 52)	P Value
Age, y	70.0 (63.2–75.9)	76.5 (71.2–82.7)	<0.001
Male	219 (56.4)	40 (76.9)	0.008
Body mass index, kg/m ²	27.1 (24.3–30.5)	25.3 (23.3–29.2)	0.069
Systolic blood pressure, mm Hg	130 (118–141)	131 (120–145)	0.428
Diastolic blood pressure, mm Hg	72.0 (64.0–80.0)	73.0 (63.0–78.5)	0.890
NYHA functional class ≥III	126 (32.5)	31 (59.6)	<0.001
Hematocrit, %	39.8 (37.0–42.4)	38.6 (35.0–41.8)	0.160
STS score	1.5 (0.9–2.4)	2.2 (1.2–2.9)	0.002
EuroSCORE II	1.4 (0.9–2.4)	2.2 (1.4–5.4)	<0.001
Past medical history			
Atrial fibrillation	41 (10.6)	15 (28.8)	<0.001
Diabetes mellitus	82 (21.1)	11 (21.2)	>0.999
Hypertension	250 (64.4)	30 (57.7)	0.630
Myocardial infarction	29 (7.5)	9 (17.3)	0.032
Aortic valve indices			
Mean pressure gradient, mm Hg	48.5 (39.2–61.8)	41.7 (33.0–50.0)	0.005
Peak aortic jet velocity, m/s	4.5 (4.0–5.0)	4.2 (3.8–4.7)	0.020
Aortic valve area index, cm ² /m ²	0.4 (0.3–0.5)	0.4 (0.3–0.5)	0.768
Valvuloarterial impedance	3.8 (3.2–4.5)	3.9 (3.4–4.9)	0.095
Bicuspid aortic valve	132 (34.0)	12 (23.1)	0.080
Aortic stenosis subtype*			0.118
High gradient	305 (81.6)	36 (72.0)	
LF-LG with reduced EF	16 (4.3)	4 (8.0)	
LF-LG with preserved EF	6 (1.6)	3 (6.0)	
NF-LG	47 (12.6)	7 (14.0)	
Intervention received			0.004
Isolated surgical AVR	284 (73.2)	27 (51.9)	
Surgical AVR + coronary artery bypass grafting	52 (13.4)	10 (19.2)	
Transcatheter AVR	52 (13.4)	15 (28.8)	
Left heart structure and function			
Left atrial volume, mL/m ² †	48.0 (38.2–59.9)	56.8 (42.8–68.3)	0.024
LV end-diastolic volume, mL/m ² †	71.0 (59.7–89.2)	81.0 (56.7–97.6)	0.475
LV end-systolic volume, mL/m ² †	20.9 (12.6–36.2)	29.9 (14.1–49.2)	0.049
LV stroke volume, mL/m ² †	47.3 (41.0–55.7)	44.6 (36.6–52.9)	0.064
LV ejection fraction, %	69.0 (58.1–79.0)	62.5 (48.5–72.5)	0.002
Maximal wall thickness, mm	15.0 (13.0–17.0)	15.0 (13.8–17.0)	0.570
LV mass, g/m ² †	87.3 (71.6–109.3)	84.0 (71.2–108.9)	0.834
Right heart structure and function			
RV end-diastolic volume, mL/m ² †	63.0 (53.0–73.5)	67.2 (53.2–81.4)	0.110
RV end-systolic volume, mL/m ² †	21.1 (15.5–27.5)	24.8 (19.4–32.3)	0.023
RV stroke volume, mL/m ² †	40.9 (33.5–48.7)	42.5 (31.2–48.8)	0.572
RV ejection fraction, %	65.3 (59.0–72.0)	61.5 (57.5–68.0)	0.025
Myocardial characteristics			
LGE	187 (48.2)	33 (63.5)	0.057
Percentage of LGE	0.0 (0.0–0.8)	0.4 (0.0–2.4)	0.004
Extracellular volume fraction, %	27.0 (25.0–29.7)	29.1 (27.0–31.5)	0.001

Values are median (interquartile range) or n (%). *Available in 95.9%. †Indexed to body surface area.

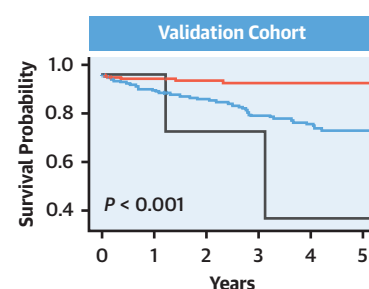
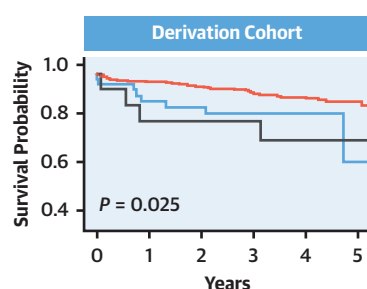
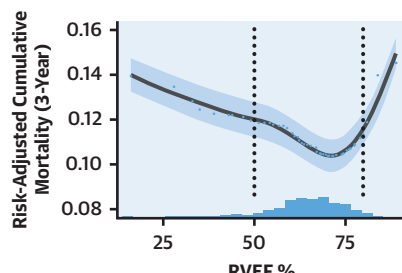
AVR = aortic valve replacement; EF = ejection fraction; EuroSCORE = European System for Cardiac Operative Risk Evaluation; LF-LG = low flow, low gradient; LGE = late gadolinium enhancement; LV = left ventricular; NF-LG = normal flow, low gradient; NYHA = New York Heart Association; RV = right ventricular; STS = The Society of Thoracic Surgeons.

VERIFICATION OF THE NONLINEAR ASSOCIATIONS AND THRESHOLD EFFECTS. To verify the clinical relevance of the RSF findings, survival was analyzed according to the thresholds observed in the partial plots (Figure 2). In the derivation cohort and using the

27% cutoff for ECV%, a markedly worse prognosis was observed with high (>27%) versus low (<27%) ECV% ($P < 0.001$). Similarly, cumulative survival was decreased in patients with high (>2%) versus low ($\leq 2\%$) LGE% ($P = 0.002$). Survival was best for

FIGURE 2 Partial Dependency Plots of the Cardiovascular Magnetic Resonance Variables and Survival Curves**A**

		Number at risk						
—	ECV% ≤ 27%	207	190	180	157	80	27	
—	ECV% > 27%	233	194	179	159	103	38	

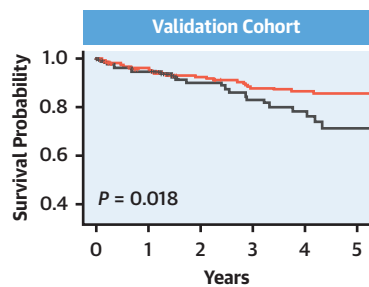
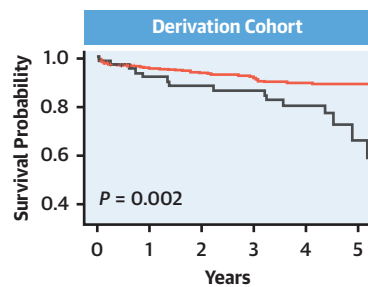
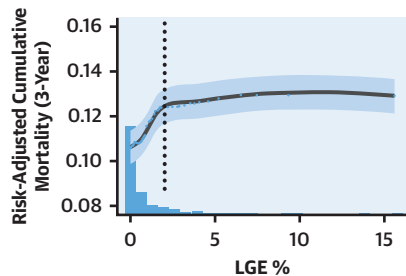
B

		Number at risk						
—	RVEF ≤ 50%	43	35	31	27	16	3	
—	RVEF 50–80%	375	332	312	274	159	57	
—	RVEF > 80%	15	11	11	11	5	3	

Partial dependency plots (**upper**) and their corresponding Kaplan-Meier curves (**lower left**, derivation cohort; **lower right**, validation cohort) for (A) ECV%, (B) RVEF, (C) LGE%, and (D) LVEDVi. The random survival forest prediction estimates were plotted with 50 points and traced by LOESS curves with 95% confidence interval. Histograms are shown at the **bottom**. Cutoff values, determined by the deflection points and normal reference range, are depicted as vertical lines. Abbreviations as in [Figure 1](#).

FIGURE 2 Continued

C



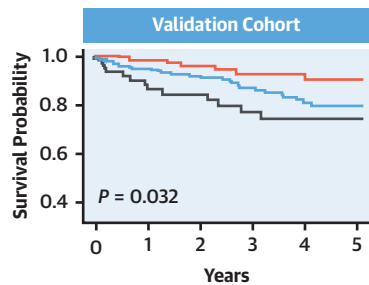
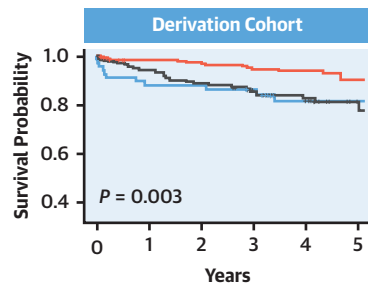
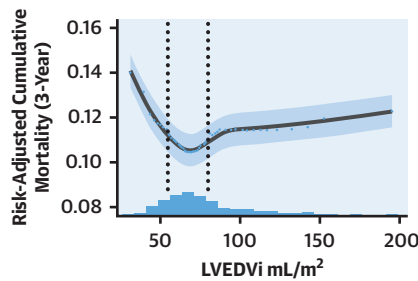
Number at risk

— LGE% ≤ 2%	370	328	308	268	151	56
— LGE% > 2%	63	53	48	45	29	9

Number at risk

— LGE% ≤ 2%	232	190	157	131	94	66
— LGE% > 2%	105	92	72	57	34	18

D



Number at risk

— LVEDVi ≤ 55mL/m ²	67	53	49	41	22	6
— LVEDVi 55–80mL/m ²	216	192	184	165	92	31
— LVEDVi > 80mL/m ²	157	139	126	110	69	28

Number at risk

— LVEDVi ≤ 55mL/m ²	192	163	135	113	71	41
— LVEDVi 55–80mL/m ²	103	85	68	53	40	28
— LVEDVi > 80mL/m ²	59	47	36	31	25	20

TABLE 2 Cox Proportional Hazards Analysis for the Variables Identified in the Random Survival Forest Model

	Derivation Cohort (n = 440)		Validation Cohort (n = 359)	
	Hazard Ratio (95% CI)	P Value	Hazard Ratio (95% CI)	P Value
Univariable Cox analysis				
ECV% >27%	2.82 (1.50-5.29)	0.001	2.50 (1.32-4.72)	0.005
RV ejection fraction				
≤50% vs. 50%-80%	2.11 (0.98-4.52)	0.056	5.16 (2.05-13.01)	<0.001
>80% vs. 50%-80%	2.90 (1.04-8.14)	0.043	13.74 (2.66-70.89)	0.002
Indexed LV end-diastolic volume				
≤55 mL/m ² vs. 55-80 mL/m ²	2.94 (1.34-6.49)	0.007	1.91 (0.87-4.18)	0.106
>80 mL/m ² vs. 55-80 mL/m ²	2.72 (1.43-5.20)	0.002	3.07 (1.29-7.32)	0.011
LGE% >2%	2.53 (1.39-4.63)	0.003	1.94 (1.11-3.39)	0.020
Adjusted Cox analysis*				
ECV% >27%	2.29 (1.20-4.37)	0.012	2.80 (1.47-5.33)	0.002
RV ejection fraction				
≤50% vs. 50%-80%	1.32 (0.57-3.04)	0.516	3.34 (1.28-8.68)	0.014
>80% vs. 50%-80%	3.12 (1.09-8.95)	0.034	32.5 (5.8-182.6)	<0.001
Indexed LV end-diastolic volume				
≤55 mL/m ² vs. 55-80 mL/m ²	2.80 (1.26-6.24)	0.012	1.45 (0.66-3.21)	0.355
>80 mL/m ² vs. 55-80 mL/m ²	2.62 (1.34-5.14)	0.005	3.47 (1.41-8.53)	0.007
LGE% >2%	2.01 (1.09-3.70)	0.026	1.34 (0.75-2.37)	0.323

*Adjusted for age, sex, atrial fibrillation, and intervention type (surgical AVR, surgical AVR + coronary artery bypass grafting, or transcatheter AVR).

CI = confidence interval; other abbreviations as in Table 1.

patients with mid-range LVEDVi (55-80 mL/m²) compared with those with either large (>80 mL/m²) or small (≤55 mL/m²) LVEDVi ($P = 0.003$). Patients with depressed (≤50%) or supranormal (>80%) RVEF had lower survival compared with the normal RVEF group (50%-80%) pairwise comparison, $P = 0.049$ and $P = 0.033$, respectively. Similar findings were observed when these thresholds were tested in Cox analyses (eg, ECV% >27%) (adjusted hazard ratio [HR]: 2.29; 95% confidence interval [CI]: 1.20-4.37; $P = 0.012$) (Table 2). In the time-varying Cox model, ECV% >27% showed an increased risk of mortality within the first 2 years post-AVR (adjusted HR: 6.95; 95% CI: 2.09-23.16; $P = 0.002$), with no significant difference thereafter (Supplemental Table 6).

INCREMENTAL PREDICTIVE VALUE OF THE MYOCARDIAL CMR VARIABLES. We examined whether the myocardial CMR variables provide additive predictive value to the clinical risk factors. Figure 3 shows the C-index of prediction models at different time points from the validation set. The baseline RSF and Cox models included only standard clinical factors (model 1), and the other model (model 2) included additional 4 CMR variables (ECV%, RVEF, LGE%, LVEDVi). The predictability of mortality was consistently higher when the CMR variables were included in the prediction models (3-year C-index: 0.778 vs 0.739 in RSF, 0.766 vs 0.731 in Cox models) (Figure 3).

ADVERSE CMR FEATURES FOR MORTALITY RISK STRATIFICATION. We further assessed whether the

combination of the myocardial CMR predictors would provide effective risk stratification. The AS-CMR risk score was built as the number of abnormal CMR features from the 4 parameters (ECV%, RVEF, LGE%, LVEDVi), in which the abnormal CMR features were defined as the higher risk strata (eg, RVEF ≤50% or >80%) compared with the lowest risk strata (eg, RVEF 50%-80%) (Supplemental Table 7). Therefore, the AS-CMR score ranged from 0 to 4.

In the derivation cohort, the cumulative 3-year mortality was highest in those with all 4 adverse CMR features (AS-CMR score 4) (cumulative incidence 43.8%; 95% CI: 0.0%-68.4%), while it was the lowest in those with 0 or 1 (cumulative incidence 3.8%; 95% CI: 1.3%-6.3%). In between, there was a stepwise increase in 3-year mortality with an increase in the AS-CMR score (Figure 4). The calibration plot of AS-CMR score is shown in Supplemental Figure 10.

When the AS-CMR score was added to clinical risk scores (Society of Thoracic Surgeons/EuroSCORE II [European System for Cardiac Operative Risk Evaluation II]), the predictability for 1-year and 3-year mortality was significantly improved based on the integrated discrimination and net reclassification improvement among the derivation cohort (Supplemental Table 8).

EXTERNAL VALIDATION IN AN INDEPENDENT COHORT. We externally validated the threshold effects and AS-CMR score in the validation cohort ($n = 359$). Similar survival patterns were observed

within the validation cohort when patients were stratified using the same thresholds (Figure 2). Particularly, the cumulative survival was again lower in patients with ECV% >27% compared with ECV% ≤27% ($P = 0.004$), with a significantly increased mortality risk with ECV% >27% in the Cox analysis (adjusted HR: 2.80; 95% CI: 1.47-5.33; $P = 0.002$) (Table 2). AS-CMR score also showed adequate risk stratification in the validation cohort, with a similar stepwise association of mortality (Figure 4).

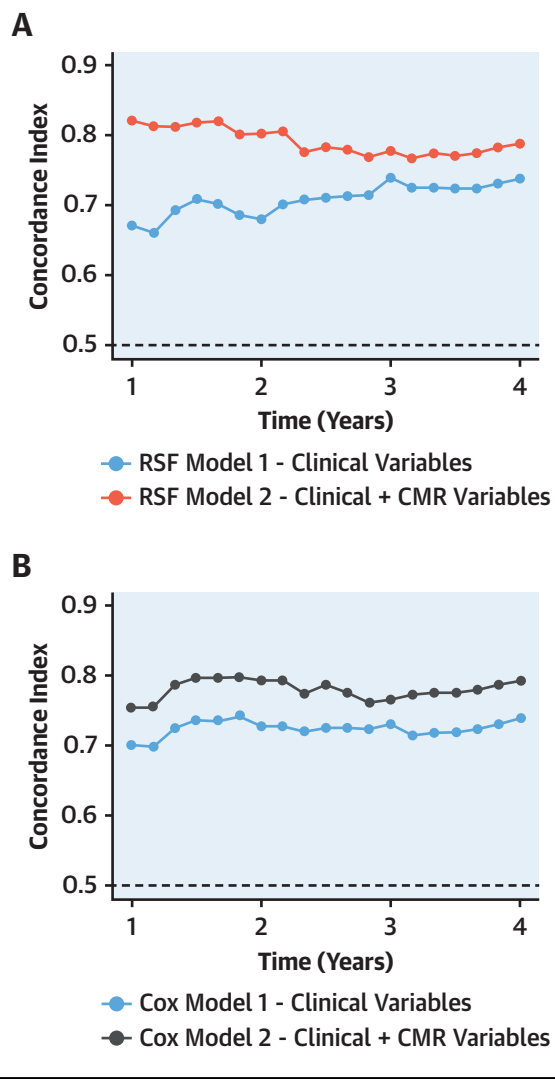
SUBGROUP ANALYSIS ACCORDING TO THE SYMPTOM STATUS AND VALVE MORPHOLOGY. For subgroup analyses, we used the combined populations of the derivation and validation cohorts (Supplemental Figures 11 and 12). In general, the 4 CMR parameters and their respective thresholds remained prognostic both in patients with no or mild symptoms (New York Heart Association [NYHA] functional class I-II) and in those with advanced symptoms (NYHA functional class III-IV) (Supplemental Figure 11). Notably, survival appeared worse with both ECV% >27% ($P = 0.051$) or LGE% >2% ($P < 0.001$) in NYHA functional class I to II patients. Regarding valve morphology, adverse CMR features were significantly associated with higher mortality in patients with tricuspid valve. The number of bicuspid patients was limited ($n = 220$) and the event rate was lower in this younger population; however, ECV% remained a significant predictor of death ($P = 0.047$) (Supplemental Figure 12).

DISCUSSION

Using machine learning, we demonstrate the powerful prognostic information of myocardial fibrosis and biventricular remodeling markers by CMR in patients with severe AS undergoing AVR. The 4 most predictive CMR markers for mortality, ECV%, LGE%, LVEDVi, and RVEF, were related to myocardial damage and displayed distinct nonlinear associations with post-AVR death. These 4 markers demonstrated clear prognostic thresholds that were robust on both internal and external validations, and can be combined into the AS-CMR score to identify patients at high risk post-AVR. Patient outcomes are therefore closely associated with myocardial health at the time of AVR, with these novel markers offering major potential in optimizing the timing of intervention and improving risk stratification.

Machine learning provides valuable methods for feature extraction and discovery of novel relationships from deeply phenotyped data (10-14). We took advantage of RSF, one of the most widely used and validated machine learning tool for time-to-event data, to discover the prognostically important CMR

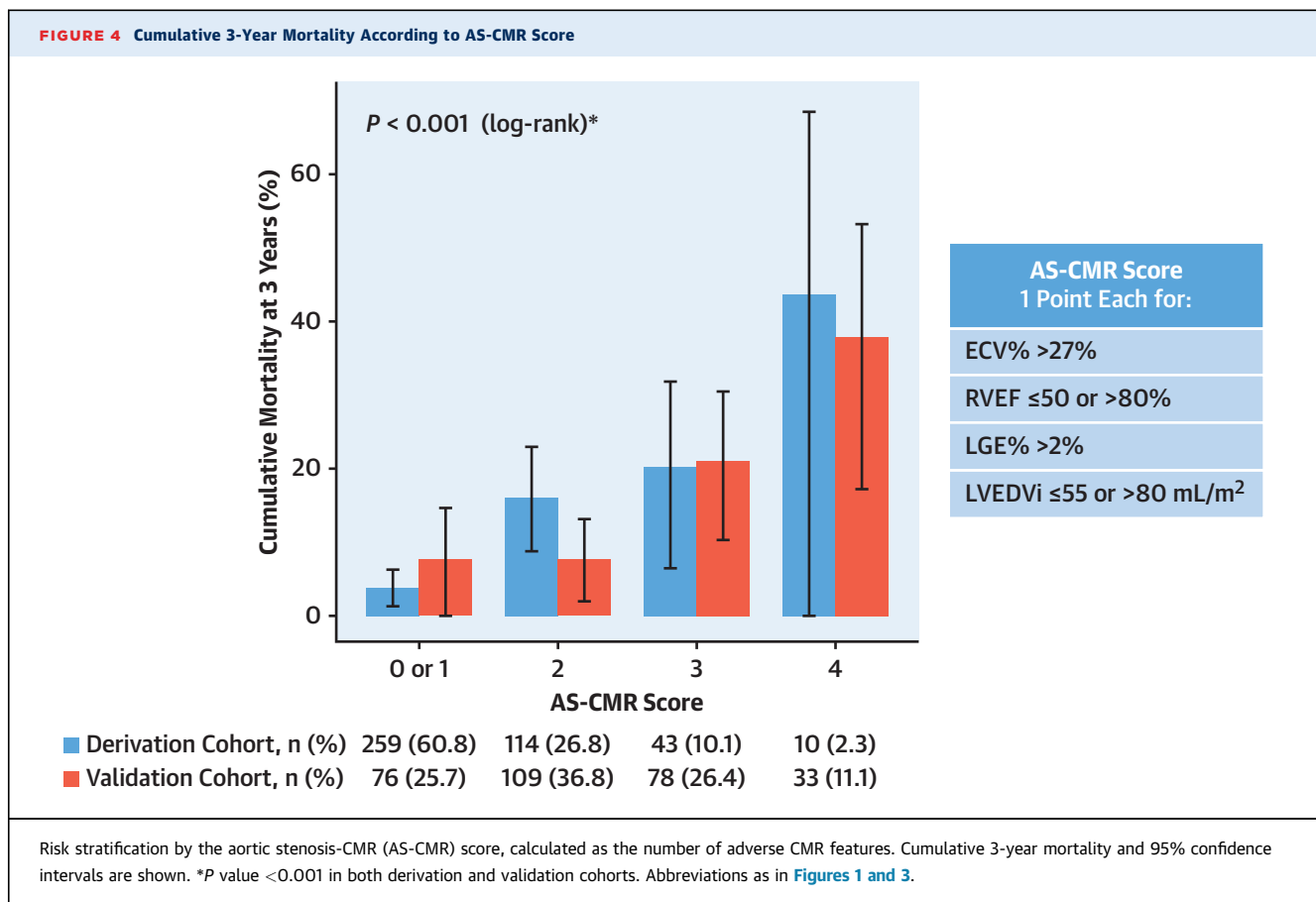
FIGURE 3 Predictive Performance of Models With and Without Myocardial CMR Variables



Predictability of random survival forest (RSF) and Cox models with or without the 4 cardiovascular magnetic resonance (CMR) variables (ECV%, RVEF, LGE%, LVEDVi). Harrell's C-index at different time points was calculated from the validation cohort. The RSF/Cox model 1 (blue line) was built with clinical factors (age, sex, atrial fibrillation, intervention type), and model 2 (red/black line) used an additional 4 CMR variables. Abbreviations as in Figure 1.

assessments (20). Importantly, RSF can uncover the nonlinear effects of variables on the outcome after adjustment for other influences (10-13), an advantage that is not readily available with conventional Cox analyses. These nonlinear relationships can be displayed intuitively with partial plots, providing clinically relevant thresholds (10-12).

Multiple studies have established the prognostic importance of LGE (replacement fibrosis) in AS (2),



while we recently reported that ECV% (diffuse fibrosis) is an independent predictor for post-AVR death (6). The predictive hierarchy from our RSF model confirmed these myocardial fibrosis markers as significant predictors of mortality, providing more powerful prognostic information than traditional AS risk factors such as peak velocity and LVEF. A limitation of previous studies with ECV% or LGE% has been the absence of clear thresholds that one might use to define LV decompensation (6). Importantly, we demonstrated a clear threshold effect for ECV% >27% that appears robust across different patient groups. Our analysis also confirmed increased mortality associated with LGE%, characterized by an increasing risk up to 2% and a plateau thereafter. This pattern may reflect the fact that ECV% quantification includes regions of late enhancement.

Among the functional and structural LV markers CMR provides, the RSF model chose LVEDVi over other conventional variables, such as LVEF or LV mass index. Unsurprisingly, patients with small LVEDVi (≤ 55 mL/m 2) had the highest proportion of paradoxical low-flow, low-gradient AS with normal ejection fraction, while patients with large LVEDVi

(>80 mL/m 2) had a high proportion of classical low-flow, low-gradient AS with reduced ejection fraction (Supplemental Table 9). Both remodeling patterns are associated with an adverse prognosis (21).

Additionally, RVEF emerged as an important prognostic marker, consistent with recent literature highlighting RV function in AS (22). Notably, studies have reported that SAVR is associated with significant RV dysfunction after surgery, whereas the RV function is generally maintained after TAVR (23). Given this, TAVR may be preferred over SAVR among those with RV dysfunction. Another interesting finding in our study was that supranormal RVEF was also associated with higher post-AVR mortality. Although the typical response to increased pulmonary artery pressure secondary to AS is RV dysfunction, the adaptation process may alternatively result in increased RV contractility (24,25). A hyperdynamic RV in AS may be associated with obstructive symptoms, elevated brain natriuretic peptide levels, and AS severity (25), suggesting its role as a marker of decompensated AS. This theory will require further validation in hypothesis-driven studies.

Echocardiography remains the gold standard modality for the assessment of valve hemodynamics; however, valve severity indices, such as peak velocity and aortic valve area, demonstrate limited association with long-term post-AVR outcomes (1). Instead, these outcomes are more closely associated with markers of myocardial health at the time of AVR (6). CMR has gained much attention in AS for the detailed assessments of myocardial health it provides. The most notable strength of CMR is that it is the only noninvasive imaging modality capable of detecting myocardial fibrosis, the major pathologic driver of LV decompensation. Markers of myocardial fibrosis and their prognostic thresholds hold promise in optimizing the timing of aortic valve intervention, especially for asymptomatic patients with severe AS. Growing data suggest that myocardial damage, including myocardial fibrosis, often begins before symptoms develop (3,4,8) and is not closely associated with hemodynamic valve assessments on echocardiography (5–8). Importantly, we demonstrate for the first time that CMR markers of fibrosis, the ECV% and LGE, provide significant prognostic information not only across the entire population, but also specifically among asymptomatic patients (patients with NYHA functional class I-II: n = 474; all-cause deaths: n = 40) (Supplemental Figure 11). This supports our hypothesis that these markers of myocardial fibrosis should be taken as objective evidence of early LV failure and that prompt valve replacement may be beneficial in patients with myocardial fibrosis even when asymptomatic. This strategy is being tested in the EVOLVED (Early Valve Replacement Guided by Biomarkers of Left Ventricular Decompensation in Asymptomatic Patients with Severe Aortic Stenosis) randomized trial (26), and the novel insight here might prove crucial when interpreting the results of this trial.

STUDY STRENGTHS. We present the largest multicenter cardiac T1-mapping study performed (n = 799), bringing together the key institutions worldwide investigating T1-mapping and other CMR approaches in AS. Moreover, rigorous testing of our findings with multiple internal validation analyses, as well as the external validation in an independent cohort, greatly enhances the generalizability of the discoveries across different international populations. Importantly, we demonstrate for the first time the clear prognostic thresholds of myocardial fibrosis—ECV% >27% and LGE% >2%—that may be readily used as a guide for clinical decisions, especially for asymptomatic patients with severe AS (n = 474) (Supplemental Figure 11), in which the benefits of early intervention are still debatable (27).

STUDY LIMITATIONS. First, the number of events in our cohort was relatively small (derivation cohort: 52 [11.8%] deaths; validation cohort: 51 [14.2%] deaths). The imbalance of the training dataset may result in suboptimal performance of the model (28), although several studies using cohorts with low event rates of 3% to 5% have reported adequate performance of RSF models (11,13), and our main results, the variable importance and partial plots, were robust across multiple internal validation analyses. Second, separate RSF analyses by each subgroup of the intervention types or sex were unavailable due to the small number of events. Third, the number of patients and events were limited in the bicuspid subgroup (13 deaths in 220 patients). We were therefore underpowered to examine the prognostic significance of CMR markers in this subgroup, which should be explored in future studies. Last, as we exclusively enrolled patients with AS undergoing AVR, the prognostic markers in patients not undergoing imminent AVR may be different.

CONCLUSIONS

We used machine learning to demonstrate that 4 CMR markers of myocardial damage (ECV%, RVEF, LGE%, LVEDVi) are important predictors of mortality in patients with severe AS undergoing AVR, with distinct thresholds and nonlinear relationships of these markers with mortality. Patient outcomes are closely associated with myocardial health at the time of AVR, with these myocardial damage markers holding major promise in optimizing the timing of AVR.

ACKNOWLEDGMENT The authors thank Jiesuck Park, MD, for his valuable comments on the RSF analysis.

FUNDING SUPPORT AND AUTHOR DISCLOSURES

The work was supported by a National Research Foundation of Korea grant funded by the Korea government (Ministry of Science and ICT; No. 2019R1A2C2084099) and a grant of the Korea Health Technology R&D Project through the Korea Health Industry Development Institute (KHIDI), funded by the Ministry of Health & Welfare, Republic of Korea (grant number HI18C2383). The authors have reported that they have no relationships relevant to the contents of this paper to disclose.

ADDRESS FOR CORRESPONDENCE: Dr Seung-Pyo Lee, Division of Cardiology, Department of Internal Medicine, Seoul National University Hospital, 101, Daehak-ro, Jongno-gu, Seoul 03080, South Korea. E-mail: sppoll@snu.ac.kr. OR Dr Marc R. Dweck, British Heart Foundation Centre for Cardiovascular Science, University of Edinburgh, 47 Little France Crescent, Edinburgh EH16 4TJ, United Kingdom. E-mail: marc.dweck@ed.ac.uk. Twitter: [@SeungPyoLee1](https://twitter.com/SeungPyoLee1).

PERSPECTIVES

COMPETENCY IN PATIENT CARE AND

PROCEDURAL SKILLS: Markers of myocardial fibrosis and ventricular remodeling detected by CMR imaging provide prognostic information in patients undergoing AVR for severe AS.

TRANSLATIONAL OUTLOOK: Future investigations

should aim to determine whether earlier AVR improves outcomes in asymptomatic patients with severe AS when CMR detects myocardial damage.

REFERENCES

1. Généreux P, Pibarot P, Redfors B, et al. Staging classification of aortic stenosis based on the extent of cardiac damage. *Eur Heart J*. 2017;38:3351–3358.
2. Musa TA, Treibel TA, Vassiliou VS, et al. Myocardial scar and mortality in severe aortic stenosis. *Circulation*. 2018;138:1935–1947.
3. Lee SP, Lee W, Lee JM, et al. Assessment of diffuse myocardial fibrosis by using MR imaging in asymptomatic patients with aortic stenosis. *Radiology*. 2015;274:359–369.
4. Chin CWL, Everett RJ, Kwiecinski J, et al. Myocardial fibrosis and cardiac decompensation in aortic stenosis. *J Am Coll Cardiol Img*. 2017;10:1320–1333.
5. Treibel TA, Lopez B, Gonzalez A, et al. Reappraising myocardial fibrosis in severe aortic stenosis: an invasive and non-invasive study in 133 patients. *Eur Heart J*. 2018;39:699–709.
6. Everett RJ, Treibel TA, Fukui M, et al. Extracellular myocardial volume in patients with aortic stenosis. *J Am Coll Cardiol*. 2020;75:304–316.
7. Lee H, Park JB, Yoon YE, et al. Noncontrast myocardial T1 mapping by cardiac magnetic resonance predicts outcome in patients with aortic stenosis. *J Am Coll Cardiol Img*. 2018;11:974–983.
8. Everett RJ, Tastet L, Clavel MA, et al. Progression of hypertrophy and myocardial fibrosis in aortic stenosis: a multicenter cardiac magnetic resonance study. *Circ Cardiovasc Imaging*. 2018;11:e007451.
9. Lee HJ, Lee H, Kim SM, et al. Diffuse myocardial fibrosis and diastolic function in aortic stenosis. *J Am Coll Cardiol Img*. 2020;13:2561–2572.
10. Dietrich S, Floegel A, Troll M, et al. Random survival forest in practice: a method for modelling complex metabolomics data in time to event analysis. *Int J Epidemiol*. 2016;45:1406–1420.
11. Hwang D, Lee JM, Yang S, et al. Role of post-stent physiological assessment in a risk prediction model after coronary stent implantation. *J Am Coll Cardiol Intv*. 2020;13:1639–1650.
12. Ingrisch M, Schoppe F, Paprottka K, et al. Prediction of (90)Y radioembolization outcome from pretherapeutic factors with random survival forests. *J Nucl Med*. 2018;59:769–773.
13. Ambale-Venkatesh B, Yang X, Wu CO, et al. Cardiovascular event prediction by machine learning: the Multi-Ethnic Study of Atherosclerosis. *Circ Res*. 2017;121:1092–1101.
14. Kwak S, Lee Y, Ko T, et al. Unsupervised cluster analysis of patients with aortic stenosis reveals distinct population with different phenotypes and outcomes. *Circ Cardiovasc Imaging*. 2020;13, e009707.
15. Moon JC, Messroghli DR, Kellman P, et al. Myocardial T1 mapping and extracellular volume quantification: a Society for Cardiovascular Magnetic Resonance (SCMR) and CMR Working Group of the European Society of Cardiology consensus statement. *J Cardiovasc Magn Reson*. 2013;15:92.
16. Messroghli DR, Moon JC, Ferreira VM, et al. Clinical recommendations for cardiovascular magnetic resonance mapping of T1, T2, T2* and extracellular volume: A consensus statement by the Society for Cardiovascular Magnetic Resonance (SCMR) endorsed by the European Association for Cardiovascular Imaging (EACVI). *J Cardiovasc Magn Reson*. 2017;19:75.
17. Baumgartner H, Falk V, Bax JJ, et al. ESC Scientific Document Group. 2017 ESC/EACTS Guidelines for the management of valvular heart disease. *Eur Heart J*. 2017;38:2739–2791.
18. O'Brien SM, Shahian DM, Filardo G, et al. The Society of Thoracic Surgeons 2008 cardiac surgery risk models: part 2-isolated valve surgery. *Ann Thorac Surg*. 2009;88:S23–S42.
19. Ishwaran H, Kogalur UB, Blackstone EH, Lauer MS. Random survival forests. *Ann Appl Stat*. 2008;2:841–860.
20. Ishwaran H, Kogalur UB, Gorodeski EZ, Minn AJ, Lauer MS. High-dimensional variable selection for survival data. *J Am Stat Assoc*. 2010;105:205–217.
21. Clavel MA, Magne J, Pibarot P. Low-gradient aortic stenosis. *Eur Heart J*. 2016;37:2645–2657.
22. Galli E, Guirette Y, Feneon D, et al. Prevalence and prognostic value of right ventricular dysfunction in severe aortic stenosis. *Eur Heart J Cardiovasc Imaging*. 2014;16:531–538.
23. Cremer PC, Zhang Y, Alu M, et al. The incidence and prognostic implications of worsening right ventricular function after surgical or transcatheter aortic valve replacement: insights from PARTNER IIA. *Eur Heart J*. 2018;39:2659–2667.
24. Aguero J, Ishikawa K, Hadri L, et al. Characterization of right ventricular remodeling and failure in a chronic pulmonary hypertension model. *Am J Physiol Heart Circ Physiol*. 2014;307:H1204–H1215.
25. Rigolli M, Sivalokanathan S, Bull S, et al. A hyperdynamic RV is an early marker of clinical decompensation and cardiac recovery in aortic stenosis with normal LV ejection fraction (letter). *J Am Coll Cardiol Img*. 2019;12:214–216.
26. Bing R, Everett RJ, Tuck C, et al. Rationale and design of the randomized, controlled Early Valve Replacement Guided by Biomarkers of Left Ventricular Decompensation in Asymptomatic Patients with Severe Aortic Stenosis (EVOLVED) trial. *Am Heart J*. 2019;212:91–100.
27. Kang DH, Park SJ, Lee SA, et al. Early surgery or conservative care for asymptomatic aortic stenosis. *N Engl J Med*. 2020;382:111–119.
28. Kaur H, Pannu HS, Malhi AK. A systematic review on imbalanced data challenges in machine learning: Applications and solutions. *ACM Comput Surv*. 2019;52:36.

KEY WORDS aortic valve stenosis, magnetic resonance imaging, random survival forest

APPENDIX For an expanded Methods and References sections and supplemental tables and figures, please see the online version of this paper.